

# RESEARCH AND DEVELOPMENT OF THE PULSE BUMP MAGNET FOR THE INJECTION SYSTEM IN CSNS/RCS

Lihua Huo<sup>†</sup>, Institute of High Energy Physics, Chinese Academy of Sciences, Beijing, 100049, P. R. China

Lei Wang, Wen Kang, Yiqin Liu, Guozhong Zhou, Jing Qiu, Mingyang Huang, Sheng Wang, the Dongguan Campus, Institute of High Energy Physics, Chinese Academy of Science Dongguan, 523770, P. R. China

## Abstract

China Spallation Neutron Source (CSNS) is a high intensity beam facility to be built in China. Its complex consists of a negative hydrogen ( $H^-$ ) linear accelerator, a rapid cycling synchrotron (RCS) accelerating the beam to 1.6 GeV energy and two beam transport lines [1], as shown in Fig. 1. The RCS accumulates protons via the injection of  $H^-$  stripping and multiple circle painting. The injection system of the RCS takes place in a 11 meter long straight section and realizes the uniform beam distributions in the synchrotron, which consists of eight pulse bump magnets and six DC magnets [2], as shown in Fig. 2. The pulse bump magnets are classified by horizontal painting bump magnets (BH1, BH2, BH3, BH4) and vertical painting bump magnets (BV1, BV2, BV3, BV4) in accordance to the direction of the beam deflection. High performance of the pulse bump magnets is crucial for efficient beam injection. The design parameters of the pulse bump magnets are indicated in Table 1.

Now, the fabrication and field measurement of all the eight pulse bump magnets were completed.

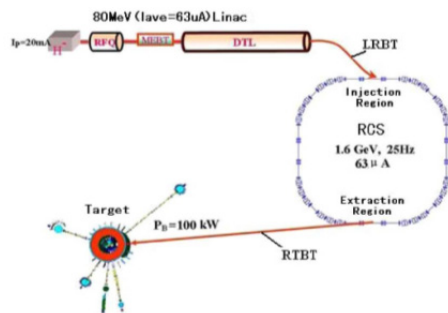


Figure 1: CSNS project accelerator complex.

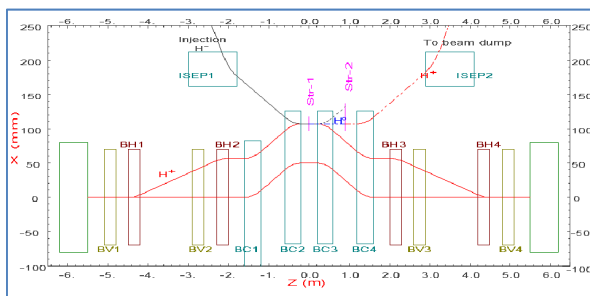


Figure 2: Schematic layout of injection.

Table 1: The Design Parameters of the Pulse Bump Magnets

Parameters	BH	BV
Injection energy (MV)	80	80
Deflection angel (mrad)	26	18.2
Max. magnetic field (T)	0.115	0.08105
Magnet effective length (mm)	300	300
Max. integral magnetic field (T·mm)	34.5	24.315
Magnet gap (mm)	186	186
Beam aperture (H/V) (mm <sup>2</sup> )	151/155	158/160
Good field range (mm)	134 (horizontal)	146.5 (vertical)
Uniformity	±1.5%	±1.5%
Current	Pulse	Pulse
Repetition rate (Hz)	25	25
Raising time (ms)	<1	<1
Flat time (μs)	50	50
Falling time (μs)	300~550	150~400

## DESIGN AND RESEARCH OF MAGNETS

In view of the narrow space in injection an asymmetric W-frame structure core is preferred, which avail lowering stray field on the injecting beam and improving the good accuracy of repetitious assembly. The core was laminated with 0.15mm thin silicon sheets to decrease the eddy current loss. In order to install the coil, it can be split into upper and lower halves. The two-turn coils are saddle and can be split into upper and lower part too.

The OPERA-3D code [3] has been used to simulate the field of the pulse bump magnet. Since the coil shape is very special, OPERA software can not automatically generate this shape coil, in order to accurately simulate as possible as the actual situation, the way of 28 pieces of conductor module seamless patchwork was used. The results BH are shown in Fig. 3. The maximum magnetic flux density in the magnet narrow yoke reached 0.98 T. The effective magnetic length is 327 mm while the core length is 220 mm. The uniformity of the integral field is about 2% within the 60% aperture. The inductance of the magnet is about  $1.94 \mu H$ . In Fig. 4, the results of BV are shown. The effective magnetic length is 328 mm while

<sup>†</sup> huolihua@ihep.ac.cn

the core length is the same as 220 mm. The uniformity of the integral field is about 2% within the 60% aperture. The inductance of the magnet is about  $2.01 \mu\text{H}$  [4]. The drawings of the bump magnet are shown in Fig. 5.

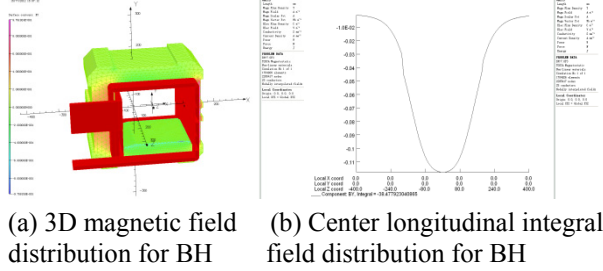


Figure 3: Field distribution for BH.

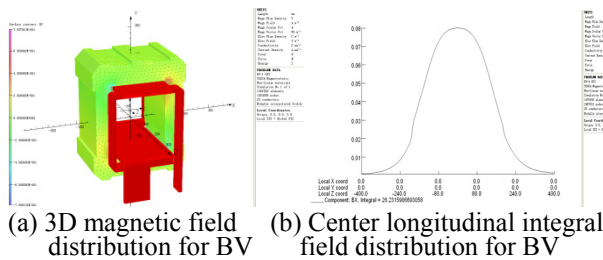


Figure 4: Field distribution for BV.

### KEY TECHNOLOGY IN FABRICATION OF MAGNETS

Because of the high average ohm heat power of the coil, the coil must be cooled with water. To avoid the influence of the cooling water pipe on the magnetic field distribution and the electric field, the coils are welded from many copper plates with cooling holes inside them, as shown in Fig. 6(a). In hydrogen furnace coil coppers soldering was done, which require high welding technology. After soldering leak detection was done on the welded coils, and it is appeared leaking for several times.

According to high radiation, the insulation of the coil requires a high tension and a high radiation resistance, so the Kapton films are applied for the coil insulation from the core. Due to special coil shape, no mould insulation casting was used after coil package. It is successful after several times trying to cast and trim. The casted coil is shown in Fig. 6(b).

In addition, the 25 Hz pulsed field induces eddy currents in the magnet components, especially in the end plates of the core. Heat generation and vibration are also of great concern. The eddy current induced in the end plates of the core is expected to be large, so some rectangular grooves are produced in the end plates of the core to cut the eddy current loops and therefore to decrease the eddy current losses.

To reduce the vibration of the coil, 12 bolts are used to pull the upper and lower parts of the coil on the core tightly. The insulation of the coil is the best key of this fixation method to solve. After the copper plates transverse drilling, only 1 mm is the distance between the ground and the current board with a high voltage. The unique insulating structural was adopted, which can meet

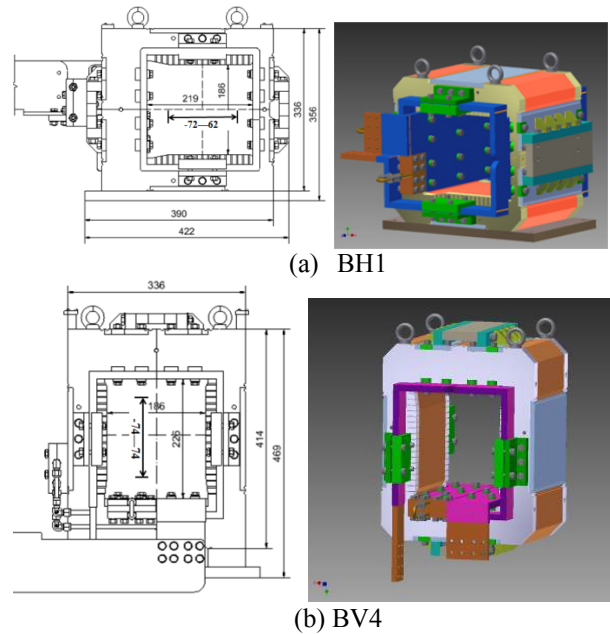
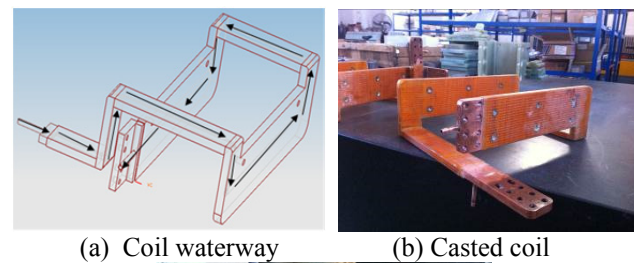


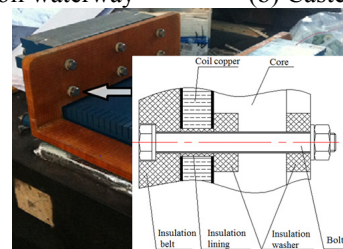
Figure 5: Front view (BH1 and BV4).

the withstanding high voltage intensity along the surface of the electric strength in 1mm creepage distance. After the assembly of the pulse bump magnet, the performance of the coil has been tested. A DC voltage of 5 kV, which is more 1.5 times higher than the full operating voltage was applied between the coil and the laminated core, and there was no obvious appearance observed within 2 minutes such as leakage current, lighter and corona. In Fig. 6(c) the fixed and insulating structure of the coil are shown.

Ceramic insulators are used to insulate the power supply from the cooling water pipes. Instead of using invar as transition connectors, the copper is directly welded with the ceramic successfully. To test the welding quality, a hydraulic pressure of  $20\text{kg}/\text{cm}^2$  was applied on the insulators and kept for 15 minutes, and there is no water leakage [5]. Figure 7 shows two completed assembly pulse bump magnets (BH1 and BV4).

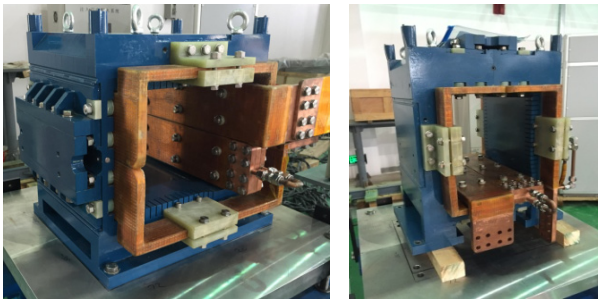


(a) Coil waterway (b) Casted coil



(c) The isolation structure of the coil

Figure 6: The structure of the coil.



(a) BH1 (b) BV4  
Figure 7: Pulse bump magnets completed.

## MAGNETIC FIELD MEASUREMENT

The measurement of the central magnetic field and integral magnetic field were done by a small searching coil and a long searching coil, respectively [6]. Figure 8 indicates the current signal and magnetic field signal measured by the long searching coil. It can be seen that the current signal curve and magnetic field signal curve conform each other very well.

The uniformity of integral magnetic field for BH1 is shown in Fig. 9(a). It can be seen that the uniformity is  $\pm 1.35\%$  in good field region. Furthermore, Fig. 9(b) shows the uniformity of integral magnetic field for BV4, in which the uniformity can reach  $\pm 1.49\%$ . The measured exciting curve of BV is shown in Fig. 10, which was synchronously measured based on magnet exciting current.

The measurement results of the two magnets are shown in Table 2, from which it can be seen the measurement results of the magnetic field meet the design specification. The measurement results of other six magnets are very similar to the two magnets.

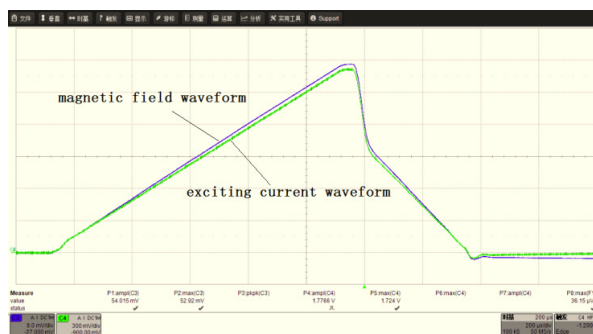
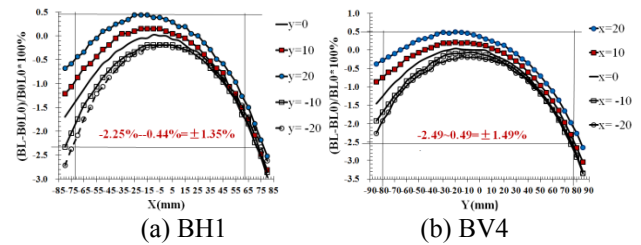


Figure 8: The current signal and magnetic field signal.

## CONCLUSION

The fabrication and measurement of four horizontal painting bump magnets and four vertical painting bump magnets for CSNS/RCS injection have been designed and successfully fabricated. In construction of the pulse bump magnets, some key technical problems on fabrication of coil were solved. A series of measurement have been done on the pulse bump magnets, whose results show that the performances of the magnets can meet the physics requirements for CSNS/RCS injection.



(a) BH1 (b) BV4  
Figure 9: The uniformity of integral magnetic field for pulse bump magnets.

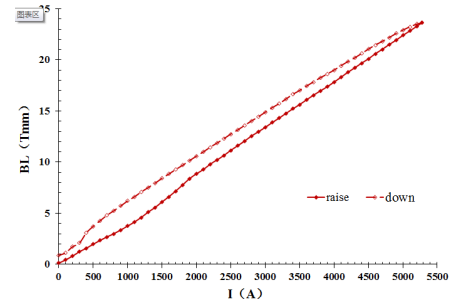


Figure 10: Exciting curves

Table 2: The Measuring Parameters Results of the Pulse Bump Magnets

Parameters	BH1	BV4
Max. magnetic field (T)	0.1152	0.08297
Magnet effective length (mm)	345.10	346.2
Max. integral magnetic field BL (T·mm)	35.70	27.39
Good field region(mm)	-62~72 (horizontal)	-74~74 (vertical)
Uniformity	$\pm 1.35\%$	$\pm 1.49\%$
Repetition rate (Hz)	25	25
Inductance ( $\mu$ H)	2.06	2.13

## REFERENCES

- [1] Jie Wei, *et al.*, "China Spallation Neutron Source: design, R&D, and outlook," *Nuclear Instruments and Methods in Physics Research A* 2009, 600, pp. 10-13.
- [2] H. S. Chen, *et al.*, "Chinese Spallation Neutron Source Preliminary Design Report (vol.)," Beijing, 2011, pp. 206-212.
- [3] Vector Fields Inc.
- [4] L. H. Huo, W. Kang, L. Wang, and Y. D. Hao, "Design of the bump magnets for the injection system of CSNS/RCS," in *The Second Conference of the Magnet and Power Supply System*, YunNan, China, 2014, pp. 34-4013.
- [5] W. Kang, L. Wang, L. H. Huo, J. X. Song, Y. D. Hao, and Y. Chen, "Design and prototype test of CSNS/RCS injection and extraction magnets," *IEEE Transactions on applied superconductivity*, JUNE 2016, 20(3), pp. 356-359.
- [6] Lihua Huo, Yiqin Liu, LeiWang, Wen Kang, and Fusan Chen, "The field measurement of the injection painting bump magnets for CSNS/RCS", *IEEE Transactions on Applied Superconductivity*, JUNE 2016, 26(4), to be published.